J. Fluid Mech. (2014), *vol.* 755, R2, doi:10.1017/jfm.2014.424

JFM RAPIDS
journals.cambridge.org/rapids

Entrainment in plane turbulent pure plumes

S. Paillat† and E. Kaminski

Institut de Physique du Globe de Paris, Sorbonne Paris Cité, Université Paris Diderot, UMR 7154 CNRS, 1 rue Jussieu, 75252 Paris CEDEX 05, France

(Received 20 May 2014; revised 26 June 2014; accepted 17 July 2014)

Turbulent jets and plumes are commonly encountered in industrial and natural environments; they are, for example, key processes during explosive eruptions. They have been the objects of seminal works on turbulent free shear flows. Their dynamics is often described with the concept of the so-called entrainment coefficient, α, which quantifies entrainment of ambient fluid into the turbulent flow. This key parameter is well characterized for axisymmetric jets and plumes, but data are scarcer for turbulent planar plumes and jets. The data tend to show that the Gaussian entrainment coefficient in plane pure plumes is about twice the value for plane pure jets. In order to confirm and to explain this difference, we develop a model of entrainment in turbulent plane jets and plumes taking into account the effect of buoyancy on entrainment, as a function of the shape of the velocity, buoyancy and turbulent shear stress profiles. We perform new experiments to better characterize the rate of entrainment in plane pure plumes and to constrain the values of the model parameters. Comparison between theory and experiments shows that the enhancement of entrainment in plane turbulent pure plumes relative to plane turbulent pure jets is well explained by the contribution of buoyancy.

Key words: geophysical and geological flows, turbulent flows

1. Introduction

Plane turbulent plumes and jets are encountered in various natural environments. Explosive basaltic eruptions, for example, often occur through fissures and produce plane (or linear) turbulent plumes on Earth (Stothers *et al.* 1986; Stothers 1989; Woods 1993) and on other terrestrial planets (Glaze, Baloga & Wimert 2011). Turbulent planar plumes can also be formed during the melting of sea ice (Wettlaufer, Worster & Huppert 1997; Widell, Fer & Haugan 2006) or can be associated with the discharge of rivers into quiescent water (e.g. Rowland, Stacey & Dietrich 2009). Classical models of natural plane plumes are based on the top-hat formalism of Morton and co-workers (Morton, Taylor & Turner 1956) and on their concept of

† Email address for correspondence: paillat@ipgp.fr

an entrainment coefficient (α) which determines the rate of entrainment and the dynamics of the flow.

The entrainment coefficient of jets and plumes is well characterized in the axysymmetric case, and various experimental studies have shown that the entrainment coefficient is about two times larger in axisymmetric plumes than in axisymmetric jets (e.g. Fischer *et al.* 1979, Papanicolaou & List 1988, Linden 2000 and Wang & Law 2002). Kaminski, Tait & Carazzo (2005) and Carazzo, Kaminski & Tait (2006) have shown how enhanced entrainment in plumes could be explained by the contribution of buoyancy. Only a few experimental studies are available for plane turbulent plumes. Since the seminal works of Rouse, Yih & Humphreys (1952) and Lee & Emmons (1961), systematic studies have confirmed a similar difference of efficiency of entrainment in plumes and jets in plane geometry. As acknowledged in early work by Kotsovinos (1977), the 'Gaussian' coefficient for pure planar plumes (no initial momentum flux), $\alpha_{plume} = 0.064 \pm 0.008$ (Kotsovinos 1975; Fischer *et al.* 1979; Ramaprian & Chandrasekhara 1989), is about twice the coefficient for pure planar jets (no initial buoyancy flux), $\alpha_{jet} = 0.035 \pm 0.010$ (Miller & Comings 1957; Bradbury 1965; Heskestad 1965; Kotsovinos 1975; Gutmark & Wygnanski 1976; Fischer *et al.* 1979; Ramaprian & Chandrasekhara 1985; Paillat & Kaminski 2014). More recently, van den Bremer & Hunt (2014) used a linear relation between α and the Richardson number to study the behaviour of turbulent planar plumes. However, no theoretical modelling of the difference of efficiency of entrainment between plane jets and plumes has been proposed so far, and the aim of this study is to do this based on the formalism developed in Priestley & Ball (1955) and Kaminski *et al.* (2005) in axisymmetric geometry. In the first part of the article we develop a theoretical model of entrainment in plane turbulent jets and plumes, and a comparison with experimental results is presented in the second part.

2. A theoretical model of entrainment in plane turbulent plumes

Planar 'pure' plumes are turbulent free shear flows driven only by their initial buoyancy flux and produced by a linear source that is infinite in one direction. The flow is bi-dimensional and can be described in an (x, z) plane, where z is the vertical direction and x lies in the horizontal plane and is normal to the direction of the linear source. Previous studies have shown that the profiles of the vertical velocity $w(x, z)$ and the reduced gravity $g'(x, z) = ((\rho_0 - \rho)/\rho)g$ in the plume (where ρ is the plume density and ρ_0 is the density of the ambient fluid) are well described, at distances $z/d > 5$ (where d is the width of the source) from the source, by Gaussian functions

$$w(x, z) = w_m(z) \exp\left(-\left[\frac{x}{b_w}\right]^2\right), \tag{2.1}$$

$$g'(x, z) = g'_m(z) \exp\left(-\left[\frac{x}{b_T}\right]^2\right), \tag{2.2}$$

where b_w and b_T are the $(1/e)$-widths of the profiles, w_m is the centreline velocity $(x = 0)$ and g'_m is the centreline buoyancy. Following Morton *et al.* (1956), the conservation equations for a pure plume are written as

$$\frac{\mathrm{d}}{\mathrm{d}z}(b_w w_m) = 2\alpha_G w_m, \tag{2.3}$$

$$\frac{\mathrm{d}}{\mathrm{d}z}\left(b_w w_m^2\right) = \sqrt{2}\, b_T\, g'_m, \tag{2.4}$$

$$\frac{\mathrm{d}}{\mathrm{d}z}\left(\sqrt{\frac{\pi}{1+\lambda^2}}\, b_T w_m g'_m\right) = 0, \tag{2.5}$$

where $\alpha_G = 1/2\, \mathrm{d}b_w/\mathrm{d}z$ is the 'Gaussian' entrainment coefficient and $\lambda = b_T/b_w$.

To model the variation of α_G between jets and plumes, we follow the same approach as in Priestley & Ball (1955) and Kaminski *et al.* (2005). We introduce $u = \overline{u} + \tilde{u}$ as the velocity along the x direction, $w = \overline{w} + \tilde{w}$ as the velocity along the z direction and $g' = \overline{g'} + \tilde{g}$ as the buoyancy, with $\overline{u}$, $\overline{w}$ and $\overline{g'}$ the time-averaged quantities, and $\tilde{u}$, $\tilde{w}$ and $\tilde{g}$ their turbulent fluctuations. At large Reynolds numbers, in a uniform environment and under the Boussinesq approximation, the time-averaged local mass, momentum and buoyancy conservation equations are written as

$$\frac{\partial \overline{u}}{\partial x} + \frac{\partial \overline{w}}{\partial z} = 0, \tag{2.6}$$

$$\overline{u}\frac{\partial \overline{w}}{\partial x} + \overline{w}\frac{\partial \overline{w}}{\partial z} = \overline{g'} + \frac{1}{\rho}\frac{\partial \tau}{\partial x}, \tag{2.7}$$

$$\overline{u}\frac{\partial \overline{g'}}{\partial x} + \overline{w}\frac{\partial \overline{g'}}{\partial z} = 0, \tag{2.8}$$

where $\tau = -\rho\overline{\tilde{u}\tilde{w}}$ is the turbulent shear stress that drives entrainment. The integration of the conservation equations (2.6)–(2.8), subject to the boundary conditions $u(x=0, z) = \tau(x=0, z) = \lim_{x\to\infty,z} \tau(x, z) = \lim_{x\to\infty,z} w(x, z) = 0$, yields

$$\frac{\mathrm{d}}{\mathrm{d}z}Q(z) = -2\lim_{x\to+\infty} \overline{u}, \tag{2.9}$$

$$\frac{\mathrm{d}}{\mathrm{d}z}M(z) = \int_{-\infty}^{+\infty} \overline{g'}(x, z)\, \mathrm{d}x, \tag{2.10}$$

$$\frac{\mathrm{d}}{\mathrm{d}z}F(z) = 0, \tag{2.11}$$

where $Q(z)$, $M(z)$ and $F(z)$ are the mass, momentum and buoyancy fluxes, respectively, defined as

$$Q(z) = \int_{-\infty}^{+\infty} \overline{w}(x, z)\, \mathrm{d}x, \tag{2.12}$$

$$M(z) = \int_{-\infty}^{+\infty} \overline{w}^2(x, z)\, \mathrm{d}x, \tag{2.13}$$

$$F(z) = \int_{-\infty}^{+\infty} \overline{w}(x, z)\overline{g'}(x, z)\, \mathrm{d}x. \tag{2.14}$$

In (2.9), the limit of $\overline{u}$ when $x \to +\infty$ quantifies entrainment in the plume, but is not known *a priori*. Morton *et al.* (1956) avoid the use of this limit through the introduction of a 'top-hat' entrainment coefficient α,

$$\frac{\mathrm{d}}{\mathrm{d}z}Q(z) = 2\alpha\frac{M}{Q}, \tag{2.15}$$

where the top-hat coefficient is related to the Gaussian coefficient through $\alpha = \sqrt{2\pi}\alpha_G$.

To obtain an explicit expression for the entrainment coefficient, we consider the conservation of the vertical kinetic energy (Priestley & Ball 1955),

$$\frac{\partial}{\partial z}\left(\frac{1}{2}\overline{w}^3\right)+\frac{\partial}{\partial x}\left(\frac{1}{2}\overline{u}\,\overline{w}^2\right)=\overline{w}\,\overline{g'}+\frac{\overline{w}}{\rho}\frac{\partial\tau}{\partial x}. \tag{2.16}$$

The integration of which, subject to the same boundary conditions as for (2.9) and (2.10), yields

$$\frac{\mathrm{d}}{\mathrm{d}z}E_c(z)=2\int_{-\infty}^{+\infty}\overline{w}\,\overline{g'}\,\mathrm{d}x+2\int_{-\infty}^{+\infty}\frac{\partial\overline{w}}{\partial x}\overline{\tilde{u}\tilde{w}}\mathrm{d}x, \tag{2.17}$$

where $E_c=\int_{-\infty}^{+\infty}\overline{w}^3\mathrm{d}x$ is the flux of kinetic energy.

We introduce three shape functions, f, h and j, for the time-averaged vertical velocity, buoyancy and turbulent stress profiles, respectively,

$$\overline{w}(x^*,z) = w_m(z)f(x^*,z), \tag{2.18}$$
$$\overline{g'}(x^*,z) = g'_m(z)h(x^*,z), \tag{2.19}$$
$$\overline{\tau}(x^*,z) = \tfrac{1}{2}\rho\, w_m(z)^2 j(x^*,z), \tag{2.20}$$

where $x^*=x/b_w(z)$, with $b_w(z)$ the length scale for the velocity profile of the plume. Six associated dimensionless integrals,

$$I_1 = \int_{-\infty}^{+\infty} f(x^*,z)\,\mathrm{d}x^*, \tag{2.21}$$
$$I_2 = \int_{-\infty}^{+\infty} f(x^*,z)^2\,\mathrm{d}x^*, \tag{2.22}$$
$$I_3 = \int_{-\infty}^{+\infty} f(x^*,z)^3\,\mathrm{d}x^*, \tag{2.23}$$
$$I_4 = \int_{-\infty}^{+\infty} \frac{\partial f(x^*,z)}{\partial x^*}j(x^*,z)\,\mathrm{d}x^*, \tag{2.24}$$
$$I_5 = \int_{-\infty}^{+\infty} h(x^*,z)\,\mathrm{d}x^*, \tag{2.25}$$
$$I_6 = \int_{-\infty}^{+\infty} f(x^*,z)\,h(x^*,z)\,\mathrm{d}x^*, \tag{2.26}$$

are then used to write the conservation of kinetic energy (2.17) as

$$\frac{\mathrm{d}}{\mathrm{d}z}E_c(z)=2F_0-\left(\frac{M}{Q}\right)^3\frac{I_4I_1^3}{I_2^3} \tag{2.27}$$

and the conservation of mass flux as

$$\frac{\mathrm{d}}{\mathrm{d}z}Q(z)=2\frac{Q}{M}\frac{\mathrm{d}}{\mathrm{d}z}M(z)-\frac{Q}{E_c}\frac{\mathrm{d}}{\mathrm{d}z}E_c(z)+\frac{M^2}{E_c}\frac{\mathrm{d}}{\mathrm{d}z}\left(\frac{QE_c}{M^2}\right). \tag{2.28}$$

By combining this last equation with (2.27) and (2.10) we obtain

$$\frac{\mathrm{d}}{\mathrm{d}z}Q(z)=2\left\{\frac{\mathscr{D}}{\mathscr{A}}Ri\left(1-\frac{1}{\mathscr{D}}\right)+\frac{\mathscr{C}}{2}+\frac{Q^2}{2M}\frac{\mathrm{d}\ln\mathscr{A}}{\mathrm{d}z}\right\}\frac{M}{Q}, \tag{2.29}$$

and hence an explicit expression for α,

$$\alpha = \frac{\mathscr{D}}{\mathscr{A}} Ri \left(1 - \frac{1}{\mathscr{D}}\right) + \frac{\mathscr{C}}{2} + \frac{Q^2}{2M} \frac{\mathrm{d} \ln \mathscr{A}}{\mathrm{d}z}, \tag{2.30}$$

where Ri, the Richardson number, is defined as

$$Ri = \frac{F_0 Q^3}{M^3}, \tag{2.31}$$

and the three other coefficients are defined as

$$\mathscr{A} = \frac{I_1 I_3}{I_2^2}, \tag{2.32}$$

$$\mathscr{C} = \frac{I_4 I_1^2}{I_3 I_2}, \tag{2.33}$$

$$\mathscr{D} = \frac{I_5 I_3}{I_6 I_2}. \tag{2.34}$$

For Gaussian velocity and buoyancy profiles, the three model parameters can be written as

$$\mathscr{A} = \sqrt{\tfrac{4}{3}}, \tag{2.35}$$

$$\mathscr{C} = \sqrt{6} I_4, \tag{2.36}$$

$$\mathscr{D} = \sqrt{\tfrac{2}{3}} \sqrt{1 + \lambda^2}. \tag{2.37}$$

The parameter $\mathscr{A}$ is then a constant, and may influence entrainment only if there is a self-similarity drift in the flow (Kaminski *et al.* 2005). Here, $\mathscr{C}$ quantifies the efficiency of turbulent entrainment driven by the Reynolds turbulent shear stress and $\mathscr{D}$ corresponds to the coupling between the velocity and buoyancy profiles, and controls the impact of buoyancy on entrainment. In the case of a pure plume considered here, the Richardson number can further be expressed as

$$Ri = \sqrt{\frac{8\pi}{1 + \lambda^2}} \frac{b_T g'_m}{w_m^2} = 2 \sqrt{\frac{4\pi}{1 + \lambda^2}} \alpha_G, \tag{2.38}$$

which leads to a simplified expression of α_G,

$$\alpha_G = \frac{\mathscr{C}}{\sqrt{8\pi}} \left(\frac{\mathscr{D}}{2 - \mathscr{D}}\right), \tag{2.39}$$

where we obtain that the efficiency of entrainment depends only on one ratio of integral profiles, the one involving the Reynolds shear stress, and on the ratio of the widths of the buoyancy and velocity profiles. To determine the values of these ratios, and to test the validity of the model, we performed an experimental study of turbulent entrainment in pure plumes.

3. Experiments

In our experiments, turbulent linear plumes are generated by the injection of salt water through a line source in a 45 cm × 30 cm × 30 cm glass tank filled with a mixture of fresh water and ethanol (between 10 and 40 weight per cent) added to match the refractive index of salted water (figure 1). For particle image velocimetry

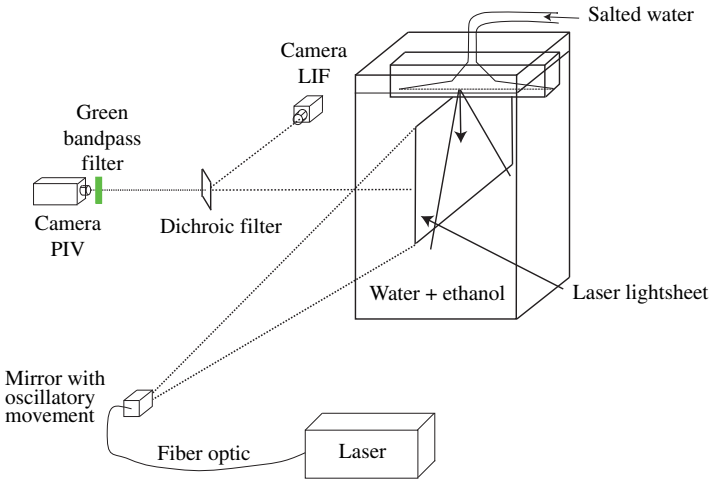

FIGURE 1. Schematic showing the experimental set-up.

Experiment	d (mm)	Q_0 (l min^{-1})	Re_0	Γ_0	$z^* = z/d$
1	1	1.57	141	0.29	60–140
2	1	1.36	123	0.36	40–150
3	1	1.93	174	0.19	80–140
4	1	1.55	140	0.49	60–140
5	1	1.59	143	0.18	80–140
6	1	1.57	142	0.22	60–120
7	1	1.87	169	0.19	40–120
8	0.5	1.57	141	0.05	150–250
9	0.5	1.50	135	0.06	130–250
10	0.5	1.47	132	0.04	130–250

TABLE 1. The experimental conditions. Here, Q_0 is the mass flow rate at the source ($z=0$), z is the distance from the source, Re_0 is the source Reynolds number and $\Gamma_0 = Ri_0/Ri_p$ is the source flux parameter calculated using the mean value of the Richardson number when the pure plume regime is reached in our experiments, $Ri_p = 0.140$.

(PIV) measurements, the fluid is seeded with glass hollow-sphere particles (LaVision 110P8) with a mean diameter of 11.7 μm and a median of 8 μm. Videos of the plumes are recorded with a camera at a frame rate of 40 Hz, and Davis™ software is used to compute the instantaneous velocity in the flow by standard PIV methods. To measure the buoyancy field, Rhodamine 6G is added to the salted water. Rhodamine 6G fluoresces at 552 nm (orange) when excited by a green laser light at 532 nm. A dichroic filter separates the 532 nm light, which is recorded by the PIV camera through a green filter, and a second camera records other wavelengths. The intensity of light is proportional to the concentration of dye and gives the concentration profile in the plume. The concentration profile has the same characteristic length as the buoyancy profile, and its centreline value is related to the centreline buoyancy through $g'_m = (c_m/c_{m_0})(F_0/Q_0)$ (Fischer *et al.* 1979).

The experimental conditions are given in table 1 for the ten experiments we performed. To generate the plumes, we used two different slot widths d of 0.5 mm and 1 mm (with aspect ratios of 370 and 185 respectively), allowing measurements

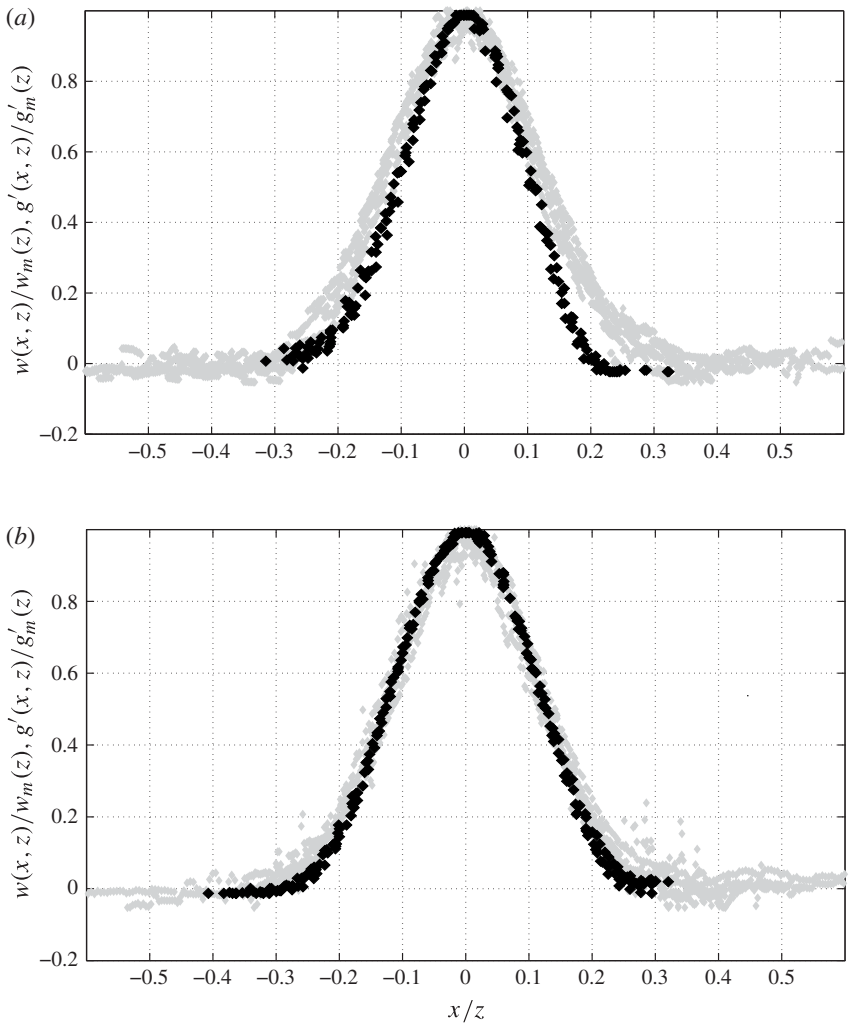

FIGURE 2. Examples of velocity profiles (black symbols) and buoyancy profiles (grey symbols) for two experiments with different widths: (*a*) $d = 1$ mm, $Re_0 = 141$, $Ri_0 = 0.041$, $60 < z^* < 140$; (*b*) $d = 0.5$ mm, $Re_0 = 132$, $Ri_0 = 0.006$, $130 < z^* < 200$.

within a range of dimensionless distances relative to the source, $z^* = z/d$, between 40 and 250. The plumes are forced plumes as their momentum flux is not zero at the source. We restrict the presentation and the discussion of the experiments to the measurements made at distances from the source at which the plumes can be considered as pure plumes. The criterion we use is that the vertical velocity remains constant with z^*.

The entrainment coefficient and the parameter λ are obtained from the velocity and concentration profiles in the pure plumes as illustrated in figure 2, where the x-axis is non-dimensionalized with the coordinate z, since b_w is proportional to z. Figure 3 shows that the centreline velocity is constant within error bars whereas the centreline concentration decreases as $1/z$ once the pure plume regime has been reached (Fischer *et al.* 1979). We find no systematic evolution of the entrainment coefficient with the

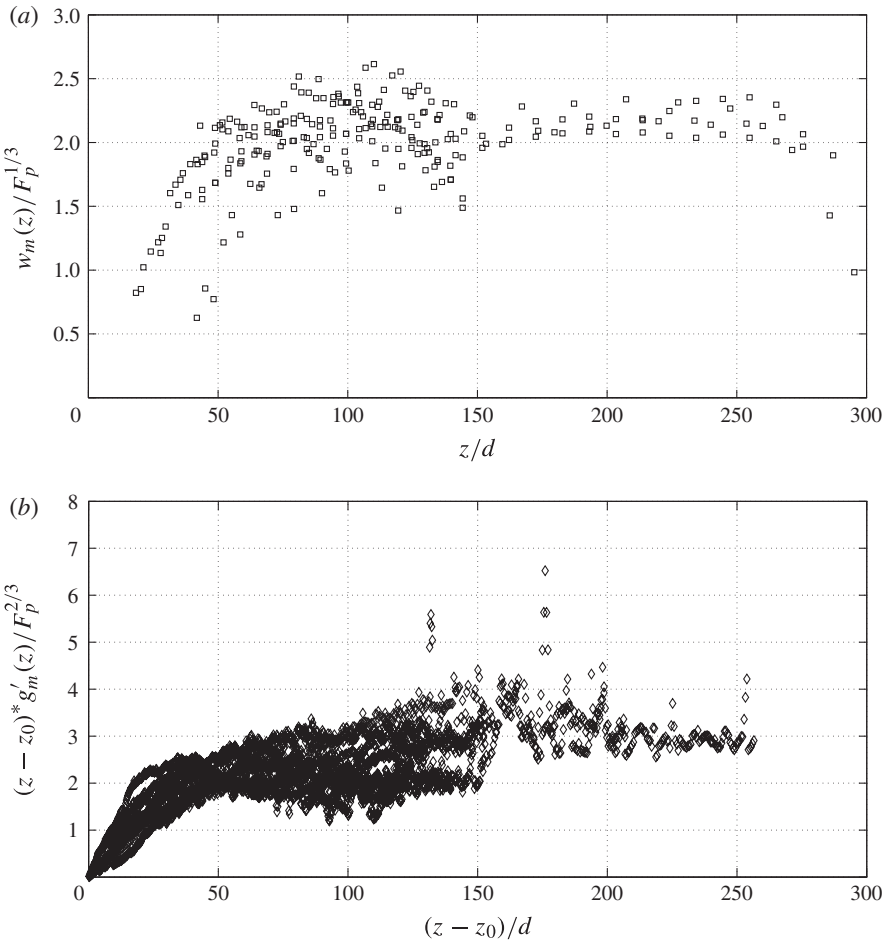

FIGURE 3. The evolution of (*a*) the centreline mean velocity and (*b*) the centreline mean buoyancy with z^* for the ten experiments. Measurements are made dimensionless using the local buoyancy flux (F_p) in the pure plume regime and the virtual plume source (z_0), determined from the theoretical expression of g'_m in pure plumes (Fischer *et al.* 1979).

source parameters, and we obtain an average value $\alpha_G = 0.071 \pm 0.006$. As expected, the value of the entrainment in the pure plumes is about two times larger that the value obtained for pure jets with the same experimental set-up, $\alpha_G = 0.04 \pm 0.010$ (Paillat & Kaminski 2014). The value of the ratio of the velocity and buoyancy profiles, λ, does not show a systematic variation as a function of the experimental conditions either, and takes an average value of 1.29 ± 0.18. This value is smaller than the one found in quasi-pure jets ($\lambda \approx 1.5$ for $Ri_0 \approx 10^{-4}$, Kotsovinos (1975) and Ramaprian & Chandrasekhara (1985)), which is consistent with an opening angle larger in pure plumes than in pure jets but shows a larger spread in the experimental data. The profiles of the Reynolds stresses for all experiments are shown in figure 4. We find that the shape and magnitude of the Reynolds shear stress do not show systematic variation with the source parameters (Ri_0, Re_0 and d) and are consistent with the profile measured in pure jets by Paillat & Kaminski (2014) with the same experimental set-up.

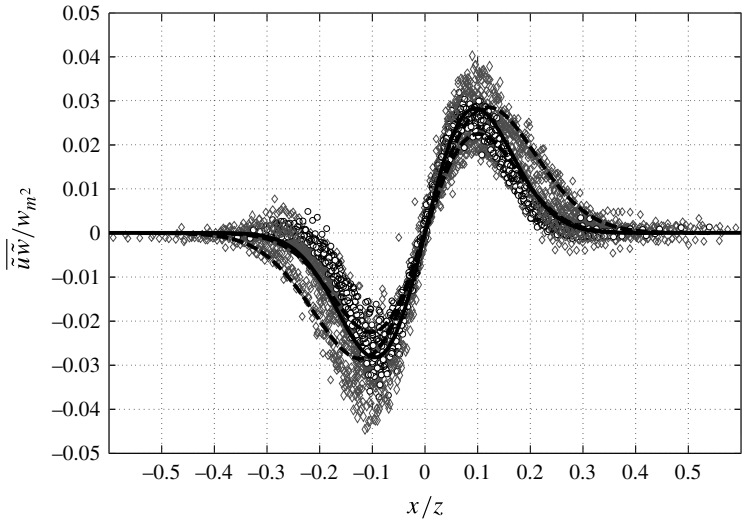

FIGURE 4. The profiles of the Reynolds stress for the ten experiments. The diamonds correspond to the slot width of 1 mm and the circles to 0.5 mm. The thick solid line is the best fit used in the model. The dashed lines are the minimum and maximum values of the Reynolds stress measured in pure jets with the same experimental set-up by Paillat & Kaminski (2014).

λ	$\mathscr{D}$	$\mathscr{C}$	α_G	$\alpha_{G_{exp}}$	Experiments
1.21 ± 0.17	1.28 ± 0.11	0.208 ± 0.030	0.074 ± 0.021	0.066 ± 0.006	RC89
1.29 ± 0.18	1.33 ± 0.12	0.198 ± 0.050	0.072 ± 0.027	0.071 ± 0.005	This study

TABLE 2. The parameters and predictions of the model for the experiments of Ramaprian & Chandrasekhara (1989) (RC89) and for the present study.

The model parameter $\mathscr{C}$ is calculated from a fit of the Reynolds shear stress profile as in Paillat & Kaminski (2014). The value we find, $\mathscr{C} = 0.198 \pm 0.050$, is close to the value calculated with the experimental data of Ramaprian & Chandrasekhara (1989), but significantly higher than the value of $\mathscr{C}$ in pure jets obtained by Paillat & Kaminski (2014), $\mathscr{C} \approx 0.150$, even if the turbulent shear stress profiles are similar in the two cases. The change of $\mathscr{C}$ is actually due to the larger opening angle in jets than in plumes (which decreases the value of the integral I_4).

The values of the model parameters and its predictions are given in table 2 for our experiments and for the study of Ramaprian & Chandrasekhara (1989), which, to the best of our knowledge, is the only published study where all the required profiles are measured, together with the experimental value of the entrainment coefficient $\alpha_G = 1/2\, \mathrm{d}b_w/\mathrm{d}z$, calculated from the opening angle of the plume. We see that the theoretical model explains, within the error bars, the higher value of the entrainment coefficient measured in pure plumes. The model predictions are consistent with both our experiments and the one of Ramaprian & Chandrasekhara (1989).

4. Conclusion

The entrainment coefficient is two times larger in pure plumes than in pure jets. We have developed a theoretical model that relates the entrainment coefficient to the local Richardson number and that explains enhanced entrainment in plumes by the contribution of buoyancy. The model introduced two dimensionless parameters, one giving the contribution of turbulent shear stress to entrainment ($\mathscr{C}$), which is also present in the case of pure jets (Paillat & Kaminski 2014), and the other one characterizing the coupling of the buoyancy and velocity profiles (λ). This second term accounts for buoyancy-induced vorticity generation, which increases the net engulfment of ambient fluid into the plume (Govindarajan 2002), and is responsible for buoyancy-enhanced entrainment in pure plumes. The two model parameters have different values in pure plumes and in pure jets and they are expected to vary with the local Richardson number in forced plumes (van den Bremer & Hunt 2014). Additional experiments would have to be performed in order to better constrain the evolution of $\mathscr{C}$ and λ as a function of Ri and to test non-Gaussian velocity and/or buoyancy profiles.

Acknowledgements

The authors thank three anonymous referees for their constructive comments and Professor J. Wettlaufer for his editorial handling of the manuscript. The experimental device was built by Y. Gamblin and R. Vazquez-Paseiro at the IPGP workshop. We thank Angela Limare for her constant help in the experiments. This study was partially funded by INSU-CNRS CT3 program.

References

BRADBURY, L. J. S. 1965 The structure of a self-preserving turbulent plane jet. *J. Fluid Mech.* **23** (1), 31–64.

VAN DEN BREMER, T. S. & HUNT, G. R. 2014 Two-dimensional planar plumes and fountains. *J. Fluid Mech.* **750**, 210–244.

CARAZZO, G., KAMINSKI, E. & TAIT, S. 2006 The route of self-similarity in turbulent jets and plumes. *J. Fluid Mech.* **547**, 137–148.

FISCHER, H. B., LIST, E. J., KOH, R. C. Y., IMBERGER, J. & BROOKS, N. H. 1979 Turbulent jets and plumes. In *Mixing in Inland and Coastal Waters*, chap. 9, pp. 315–389. Ed. Academic Press.

GLAZE, L. S., BALOGA, S. M. & WIMERT, J. 2011 Explosive volcanic eruptions from linear vents on Earth, Venus, and Mars: comparisons with circular vent eruptions. *J. Geophys. Res.* **116**, 1011.

GOVINDARAJAN, R. 2002 Universal behavior of entrainment due to coherent structures in turbulent shear flow. *Phys. Rev. Lett.* **88** (13), 134503-1.

GUTMARK, E. & WYGNANSKI, I. 1976 The planar turbulent jet. *J. Fluid Mech.* **73** (Part 3), 465–495.

HESKESTAD, G. 1965 Hot-wire measurements in a plane turbulent jet. *Trans. ASME J. Appl. Mech.* **32**, 721–734.

KAMINSKI, E., TAIT, S. & CARAZZO, G. 2005 Turbulent entrainment in jets with arbitrary buoyancy. *J. Fluid Mech.* **526**, 361–376.

KOTSOVINOS, N. E. 1975 A study of the entrainment and turbulence in a plane buoyant jet. PhD thesis, California Institute of Technology.

KOTSOVINOS, N. E. 1977 Plane turbulent buoyant jets. Part 1. Integral properties. *J. Fluid Mech.* **81** (1), 25–44.

LEE, S. L. & EMMONS, H. W. 1961 A study of natural convection above line fires. *J. Fluid Mech.* **11** (3), 353–368.

LINDEN, P. F. 2000 Convection in the environment. In *Perspectives in Fluid Dynamics: A Collective Introduction to Current Research*, chap. 6, pp. 289–345. Cambridge University Press.

MILLER, D. R. & COMINGS, E. W. 1957 Static pressure distribution in the free turbulent jet. *J. Fluid Mech.* **3** (1), 1–16.

MORTON, B. R., TAYLOR, G. & TURNER, J. S. 1956 Turbulent gravitational convection from maintained and instantaneous sources. *Proc. R. Soc. Lond.* A **234** (1196), 1–23.

PAILLAT, S. & KAMINSKI, E. 2014 Second-order model of entrainment in planar turbulent jets at low Reynolds number. *Phys. Fluids* **26**, 045110.

PAPANICOLAOU, P. N. & LIST, E. J. 1988 Investigations of round turbulent buoyant jets. *J. Fluid Mech.* **195**, 341–391.

PRIESTLEY, C. H. B. & BALL, F. K. 1955 Continuous convection from an isolated source of heat. *Q. J. R. Meteorol. Soc.* **81**, 144–157.

RAMAPRIAN, B. R. & CHANDRASEKHARA, M. S. 1985 LDA measurements in plane turbulent jets. *J. Fluids Engng, Trans. ASME* **107**, 264–271.

RAMAPRIAN, B. R. & CHANDRASEKHARA, M. S. 1989 Measurements in vertical plane turbulent plumes. *J. Fluids Engng, Trans. ASME* **111**, 69–77.

ROUSE, H., YIH, C. S. & HUMPHREYS, H. W. 1952 Gravitational convection from a boundary source. *Tellus* **4**, 201–210.

ROWLAND, J. C., STACEY, M. T. & DIETRICH, W. E. 2009 Turbulent characteristics of a shallow wall-bounded plane jet: experimental implications for river mouth hydrodynamics. *J. Fluid Mech.* **627**, 423–449.

STOTHERS, R. B. 1989 Turbulent atmospheric plumes above line sources with an application to volcanic fissure eruption on the terrestrial planets. *J. Atmos. Sci.* **46** (17), 2662–2670.

STOTHERS, R. B., WOLFF, J. A., SELF, S. & RAMPINO, M. R. 1986 Basaltic fissure eruptions, plume heights and atmospheric aerosols. *Geophys. Res. Lett.* **13** (8), 725–728.

WANG, H. & LAW, A. W.-K. 2002 Second-order integral model for a round turbulent buoyant jet. *J. Fluid Mech.* **459**, 397–428.

WETTLAUFER, J. S., WORSTER, G. M. & HUPPERT, H. E. 1997 Natural convection during solidification of an alloy from above with application to the evolution of sea ice. *J. Fluid Mech.* **344**, 291–316.

WIDELL, K., FER, I. & HAUGAN, P. M. 2006 Salt release from warming sea ice. *Geophys. Res. Lett.* **33**, L12501.

WOODS, A. W. 1993 A model of the plumes above basaltic fissure eruptions. *Geophys. Res. Lett.* **20**, 1115–1118.